A Eukaryotic Protein, NOP-1, Binds Retinal To Form an Archaeal Rhodopsin-like Photochemically Reactive Pigment†

Jennifer A. Bieszke, Elena N. Spudich, Kenneth L. Scott, Katherine A. Borkovich, and John L. Spudich*

Department of Microbiology and Molecular Genetics, The University of Texas Medical School, Houston, Texas 77030

Received July 13, 1999; Revised Manuscript Received August 16, 1999

ABSTRACT: The *nop-1* gene from *Neurospora crassa* is predicted to encode a seven-helix protein exhibiting conservation with the rhodopsins of the archaeon *Halobacterium salinarum*. In the work presented here we have expressed this gene heterologously in the yeast *Pichia pastoris,* obtaining a relatively high yield of 2.2 mg of NOP-1 protein/L of cell culture. The expressed protein is membrane-associated and forms with *all-trans* retinal a visible light-absorbing pigment with a 534 nm absorption maximum and ∼100 nm half-bandwidth typical of retinylidene protein absorption spectra. Its λ_{max} indicates a protonated Schiff base linkage of the retinal. Laser flash kinetic spectroscopy demonstrates that the retinal-reconstituted pigment undergoes a photochemical reaction cycle with a near-UV-absorbing intermediate that is similar to the M intermediates produced by transient Schiff base deprotonation of the chromophore in the photocycles of bacteriorhodopsin and sensory rhodopsins I and II. The slow photocycle (seconds) and long-lived intermediates (M and O) are most similar to those of the phototaxis receptor sensory rhodopsin II. The results demonstrate a photochemically reactive member of the archaeal rhodopsin family in a eukaryotic cell.

Vitamin A aldehyde (retinal) is used for absorption of light by two distinct families of phototransducers. First, visual rhodopsins are the photosensory pigments found in eyes throughout the animal kingdom (*1*). Second, prokaryotic archaeal rhodopsins are light-driven ion transporters (*2*−*4*) and photosensory receptors (*5*) in phototactic halophilic archaea. Both visual and archaeal rhodopsins are characterized by a seven transmembrane helix structure that forms a pocket in which retinal is covalently linked as a protonated Schiff base to a lysine in the seventh helix. Despite this similar topology there is no compelling primary sequence homology between the two families, which may have converged from two independent origins. In particular, the highly conserved 22-residue retinal-binding pocket of the archaeal rhodopsins is not convincingly conserved in visual pigments. Further, the retinal isomeric configurations and ring/chain conformations differ in visual pigments and in archaeal rhodopsins (11-*cis* vs *all-trans* and ring/chain 6-s-*cis* vs 6-s-*trans*, respectively; *6*).

Many photosensory responses of diverse organisms have been documented for which photoreceptors accounting for the full spectral range of sensitivity have not been identified. Examples are phototaxis and other photomotility responses (*7*, *8*) and light entrainment of circadian rhythms in microorganisms and higher animals (*9*, *10*). There is evidence suggesting that retinal may be the chromophore for some of these nonvisual photosensory phenomena. Restoration of phototaxis by retinal addition to pigment-deficient cells of *Chlamydomonas reinhardtii* first indicated a retinal-containing photoreceptor in a eukaryotic microorganism (*11*). Similar evidence has been reported for phototaxis by the fungus *Allomyces reticulatus* (*12*). Several laboratories have subsequently studied motility behavior of pigment-deficient *C. reinhardtii* cells reconstituted with retinal isomers and analogues. These studies confirmed the retinylidene chromophore in *C. reinhardtii* phototaxis and moreover demonstrated an archaeal-like retinal configuration and ring/chain conformation in the *C. reinhardtii* photoreceptor (*13*−*15*). A protein that forms a covalent attachment with radioactive retinal upon treatment with a reducing agent has been proposed to be the *C. reinhardtii* photoreceptor (*16*). This protein, named chlamyrhodopsin, does not exhibit the characteristic seven-helix structure or extensive regions of identity with either the archaeal or visual rhodopsin families and therefore was proposed to be a new type of sensory photoreceptor (*16*).

Recently, a gene predicted to encode a protein exhibiting conservation with the archaeal rhodopsins has been identified in *Neurospora crassa* (*nop-1*; *17*). Several responses to blue light have been documented in this organism (*18*), and a mutant selection scheme has been developed by coupling blue light signaling to amino acid transport in order to identify genes involved in photosignal transduction (*19*). Several proteins involved in blue light signal transduction, including possible flavoprotein photoreceptors, have been identified using this and other approaches, but the number and type of photosensory receptors responsible for *N. crassa* responses to light remain to be determined (*18*).

In the work presented here we have expressed the *nop-1* gene heterologously in the yeast *Pichia pastoris* and show that its protein product forms with *all-trans* retinal a visible light-absorbing pigment with absorption properties and a

† The work was supported by National Institutes of Health Grant R01GM27750 (to J.L.S.).

* To whom correspondence should be addressed. Tel: 713-500-5458. Fax: 713-500-5499. E-mail: spudich@utmmg.med.uth.tmc.edu.

10.1021/bi9916170 CCC: $18.00
Published on Web 10/07/1999

photochemical reaction cycle characteristic of the archaeal sensory rhodopsins. The results extend the family of photochemically reactive archaeal rhodopsin pigments to the eukaryotic domain.

MATERIALS AND METHODS

Materials. The *P. pastoris* expression plasmid and recipient strain were from Invitrogen (Carlsbad, CA). Yeast nitrogen base without amino acids, yeast extract, and proteose peptone were from Difco, and restriction endonucleases were from Promega (Madison, WI). *Pfu* polymerase used in PCR[1] amplification was from Stratagene (La Jolla, CA). *All-trans* retinal was from Sigma (St. Louis, MO). 9-*cis*, 11-*cis*, and 13-*cis* retinal were prepared as described (*20*). Synthetic oligonucleotides were from Genosys (The Woodlands, TX).

Plasmid Construction. The *N. crassa* opsin gene *nop-1* (Accession Number AF135863; *17*) was cloned into the *Eco*RI site of the pHIL-S1 plasmid downstream from the *P. pastoris* alcohol oxidase 1 (AOX1) gene promoter and the acid phosphatase (PHOI) secretion signal (S) following a strategy used successfully for bovine opsin (*21*). *Eco*RI sites were created at the 5′ and 3′ ends of the opsin gene, and a hexahistidine epitope was placed at the C-terminus using the polymerase chain reaction (PCR) and the following primers: forward (5′ GCGAATTCGAAACAGGCCACCG-CACTCTATGG) and reverse (5′ GCGAATTCTCAGTG-GTGGTGGTGGTGGCTCTCC). The insert in the resulting plasmid NoppHIL-S1 was confirmed by DNA sequencing.

Expression of NOP-1 in P. pastoris. The *P. pastoris* strain GS115 grown on medium A [yeast extract (10 g/L), proteose peptone (20 g/L), and dextrose (20 g/L)] was the recipient strain for electroporation of NoppHIL-S1 (containing the *nop-1* gene) and of pHIL-S1 (the plasmid without the *nop-1* insert) as a control. Plasmids were linearized using *Stu*I, and 1 μg of DNA was electroporated as described (*21*). Transformants were screened for integration of the NoppHIL-S1 and pHIL-S1 plasmids into the genome by PCR and Southern analysis. Six NoppHIL-S1 transformants were grown in 25 mL cultures following the manufacturer's instructions to check for NOP-1 protein expression by immunoblot analysis. One NoppHIL-S1 transformant (L4) was chosen and grown on a large scale. Briefly, 25 mL of medium B [yeast nitrogen base without amino acids (13.4 g/L), biotin (0.4 mg/L), and glycerol (1.0%, v/v)] was inoculated, and the culture was incubated at 30 °C with shaking at 300 rpm until $A_{600} = 10.0$. An aliquot (0.75 mL) was used to inoculate 250 mL of medium B and incubated at 30 °C with shaking until $A_{600} = 3.6$. The cells were pelleted by centrifugation at 1500*g* for 5 min at 4 °C and resuspended in 900 mL of medium C [yeast nitrogen base without amino acids (13.4 g/L), biotin (0.4 mg/L), and methanol (0.5%, v/v)] to obtain a final $A_{600} = 1.0$. Additional methanol (4.5 mL) was added to the culture after 24 h incubation. After an additional 24 h of growth, the culture was harvested by centrifugation at 1500*g* for 5 min at 4 °C. The supernatant was subsequently removed, and the cell pellet was stored at −20 °C. A large-scale culture of cells containing pHIL-S1 was prepared in the same manner as a control.

Preparation of Membranes from P. pastoris Cells and Immunoblotting. Cell pellets harvested from the 900 mL cultures were washed once with ice-cold, sterile water and centrifuged at 1500*g* for 5 min at 4 °C and subsequently washed a second time with buffer A (7 mM NaH_2PO_4, pH 6.5, 7 mM EDTA, 7 mM dithioerythritol, 1 mM PMSF). The cells were finally resuspended in one pellet volume of Buffer A. Aliquots (1 mL) were combined with acid-washed 0.5 mm glass beads (~1 mL) and disrupted with three 1-min pulses, and two 90-s pulses using a minibead beater (Biospec Products, Inc., Bartlesville, OK) at 4 °C. The extracted material was centrifuged at 1500*g* for 5 min at 4 °C, and the supernatants were collected. The pellets containing beads and cells were combined with 0.7 mL of buffer A and disrupted for an additional 90 s. The tubes were centrifuged at 750*g*, and the supernatant was collected and combined with the supernatant collected previously to yield the cell lysate. The cell lysate was layered on a sucrose cushion (70% w/v in buffer A) and centrifuged with no braking at 92000*g* for 1 h at 4 °C in a SW27 swinging bucket rotor (Beckman, Fullerton, CA). A visible band composed of cellular membranes, located at the interface between the lysate and sucrose cushion, was collected and stored at 4 °C and used as the membrane preparation in this study.

Immunoblot analysis of cell lysates and membrane preparations containing 35 μg of protein was conducted by SDS−PAGE and imunoblotting as previously described (*22*). Anti-6× His monoclonal antibody (Clontech, Palo Alto, CA) at a 1:3000 dilution was used as the primary antibody, and an anti-mouse IgG HRP conjugate (Bio-Rad, Hercules, CA) at a 1:5000 dilution was used as the secondary antibody. Reactive bands were visualized using ECL Western blot detection reagents (Amersham, Piscataway, NJ).

Spectroscopy. Absorption spectra for analysis of NOP-1 in *P. pastoris* membranes were measured in membranes pelleted and resuspended at 2−5 mg/mL in 20 mM NaH_2PO_4, pH 6.5, and 1 mM PMSF. *All-trans* retinal from 0.14 to 0.50 mM ethanolic stocks was added (2−5 μL) to a 2 mL suspension of membranes to a final concentration ranging from 3.5 to 4.5 × 10^{-7} M measured against an unreconstituted suspension. Spectra were recorded on a SLM-Aminco DW2000 double beam spectrophotometer (Spectronic Instruments, Rochester, NY) with a path length of 1 cm. Flash-induced absorption changes were measured with a laboratory-constructed cross-beam kinetic spectrophotometer (*23*) with a Surelite I Nd:YAG laser (Continuum, Santa Clara, CA) providing an actinic flash with these parameters: 6 ns, 532 nm, 40 mJ. The flashing frequency was 0.08 Hz, and 128 transients were acquired at constant temperature (23 °C) and averaged to produce each trace. Amplitudes and $t_{1/2}$ values were calculated using a double exponential curve-fitting algorithm from the program Igor (WaveMetrics, Lake Oswego, OR).

Reconstitution, Extraction, and HPLC. *P. pastoris* membrane samples were prepared as described above for spectrophotometric analysis. Retinal isomers (2−5 μL) were added to 2 mL membrane suspensions to a final concentration of 4.7 × 10^{-7} M. The incubation was continued for 4 h at room temperature in the dark, and the absorption spectra were recorded at 10 min intervals. Darkness was maintained

[1] Abbreviations: PCR, polymerase chain reaction; NR_{534}, the unphotolyzed state of the pigment formed by addition of *all-trans* retinal to the NOP-1 protein; M, N, and O, spectrally distinct intermediates of the photochemical reaction cycle of NR_{534}.

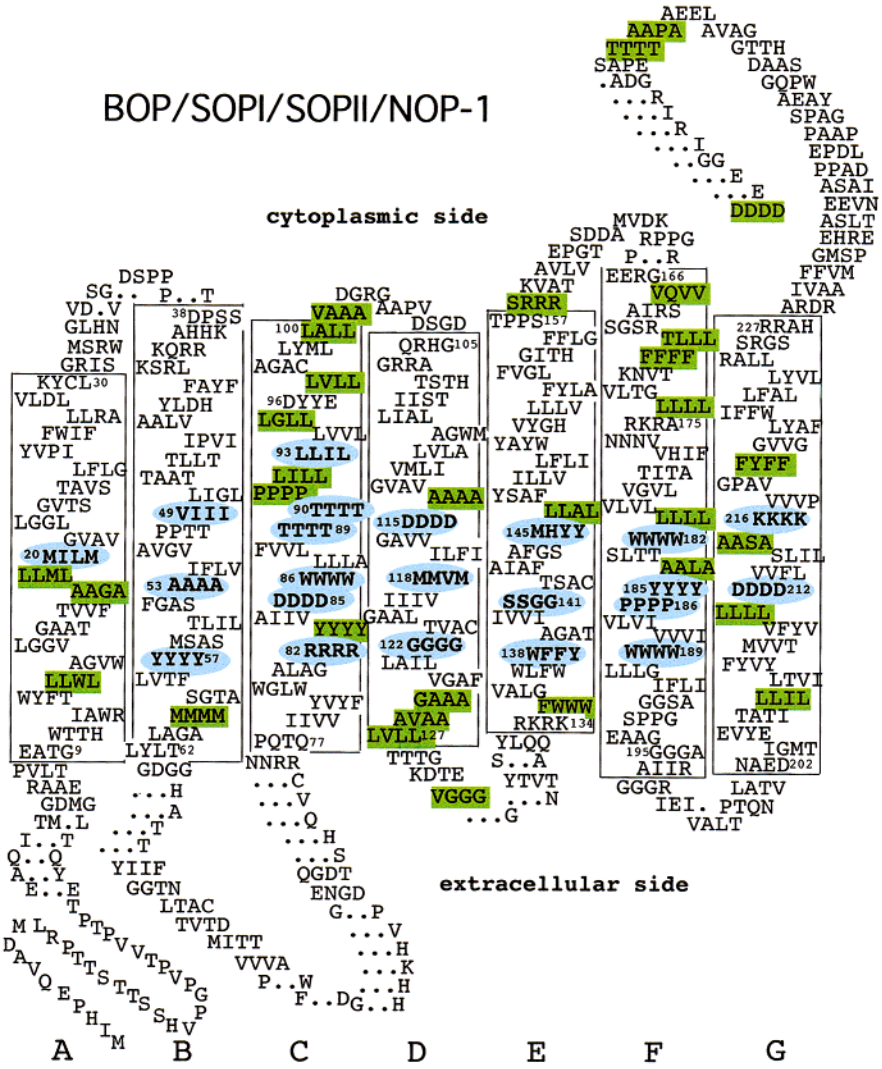

FIGURE 1: Structurally based alignment of NOP-1 with archaeal rhodopsins. Residue numbers and helix boundaries are based on those of bacteriorhodopsin (*2*). Residues forming the retinal-binding pockets of archaeal rhodopsins are indicated in blue. Residues in NOP-1 identical to at least two of the three archaeal rhodopsin residues at the corresponding position are indicated in green. Dots indicate gaps in the corresponding sequence and for simplicity are omitted in the predicted N-terminal residues of NOP-1 that extend beyond the archaeal rhodopsin sequences.

throughout the following procedures. The membrane suspensions were pelleted by centrifugation and resuspended in 200 μL of the same buffer. Retinal was then extracted from the sample using the ethanol/hexane procedure described (*24*) where the reagent amounts were scaled up to accommodate the greater starting volume of the membrane suspension. Retinal isomers were identified immediately after extraction by high-performance liquid chromatography (HPLC) using a Whatman (Meldstone, England) 25 cm Partisil 5 silica gel column and elution with 8% ethyl acetate in hexane (v/v) at a flow rate of 0.5 mL/s. To reconfirm assignments of *all-trans* and 9-*cis* retinal made in Figure 5, these isomers were co-injected with the extracted samples.

RESULTS AND DISCUSSION

Membrane Topology Alignment of NOP-1 with Archaeal Rhodopsins. The predicted amino acid sequence of NOP-1 was noted previously to exhibit high similarity to archaeal rhodopsins (*17*). Alignment with bacteriorhodopsin and sensory rhodopsins I and II based on the hydropathy-predicted topology of NOP-1 in the membrane indicates nearly complete conservation of the chromophore binding pocket residues (indicated in blue in Figure 1), which are ~80% identical to each member of the archaeal rhodopsin family (*17*). This extent of identity is comparable to that shown by the archaeal rhodopsins with each other (Figure 1). Furthermore, many additional residues in NOP-1 are identical to those of two or more of the archaeal rhodopsins (indicated in green in Figure 1). Most of these lie within the predicted transmembrane domain of NOP-1 including regions predicted to be outside of the chromophore contact residues.

Two residues of known functional importance in both transporters and sensors, the lysine that forms a protonated Schiff base with retinal and the Schiff base primary counterion residue, are conserved in NOP-1. These are Lys216 in helix G (numbered according to BR; Lys263 in NOP-1) and Asp85 in helix C (Asp131 in NOP-1). Four residues in BR involved in proton release (Glu194 and Glu204 near the extracellular surface) and in proton uptake (Thr46 and Asp96 near the cytoplasmic surface) are substituted nonconservatively in both SRI and SRII. Three of the four are conserved in NOP-1 (except for Glu194 which is a glycine residue).

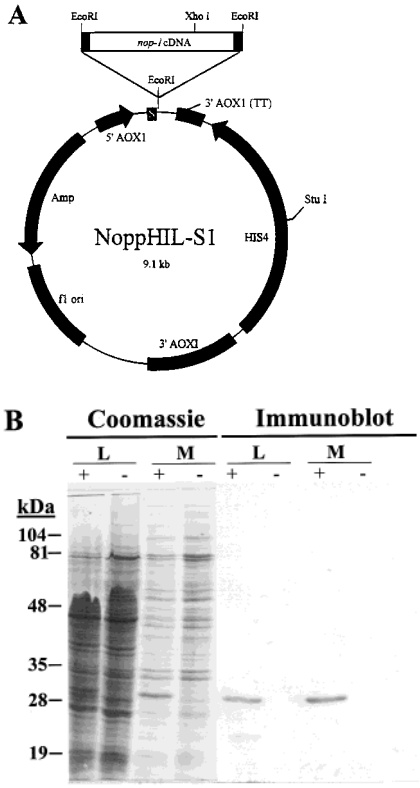

FIGURE 2: (A) *P. pastoris* expression vector constructed for expression of the *nop-1* gene. Key: 5′AOX1, the *P. pastoris* alcohol oxidase 1 gene promoter; S, secretion signal-encoding sequence of the *P. pastoris* acid phosphatase 1 gene; AOX1 (TT), the native transcription termination and polyadenylation signal from the alcohol oxidase 1 gene; HIS4, the *P. pastoris* gene encoding histidinol dehydrogenase; 3′AOX1, sequence from the AOX1 gene 3′ to the transcription terminator; f1 ori, the bacteriophage f1 origin of replication; Amp, ampicillin resistance gene. (B) Characterization of transformant membranes from *P. pastoris* with and without NOP-1. Sample proteins were electrophoretically separated on a 12.5% SDS−polyacrylamide gel and visualized by Coomassie staining in lanes 1−4 and by immunoblotting with the 6× His monoclonal antibody in lanes 5−8. Key: L, whole cell lysate; M, membrane preparation; +, transformant L4 containing the *nop-1* gene; −, control transformant V1 containing vector without the *nop-1* gene.

Therefore, NOP-1 is more similar to BR than are SRI or SRII in its conservation of these residues; however, as will be addressed below, its photochemistry is more similar to that of the sensory rhodopsins.

Expression of nop-1 in P. pastoris. The methylotrophic yeast, *P. pastoris*, was chosen as a host for expression of the *nop-1* gene because it was successfully used for functional heterologous expression of the bovine opsin gene (*21*). The vector NoppHIL-S1 was constructed with the *nop-1* gene preceded by the *PHO1* signal sequence (S, Figure 2A), a native secretion signal expected to target the opsin to the plasma membrane. In our construct, the insertion point of *nop-1* is in-frame with the signal sequence and immediately downstream from the secretion signal cleavage site (*25*). The N-terminal sequence of the mature NOP-1 protein encoded by this construct begins with ArgGluPhe, as did the bovine rhodopsin expressed similarly (*21*), followed by GluThrGly, which is just prior to the entry of the predicted helix A into the membrane as drawn in Figure 1. A sequence encoding six histidine residues at the C-terminus of NOP-1 was included to provide an immunoreactive epitope.

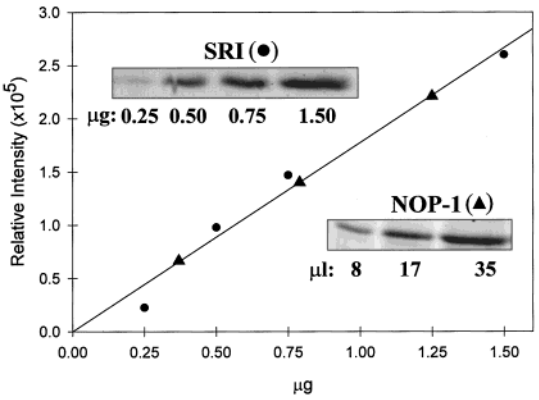

FIGURE 3: Quantitation of NOP-1 expression. Upper inset and circles: Coomassie stain densities of known amounts of sensory rhodopsin I. Lower inset and triangles: densities of three dilutions of a NOP-1 membrane preparation placed on the linear regression line to the sensory rhodopsin I calibration points.

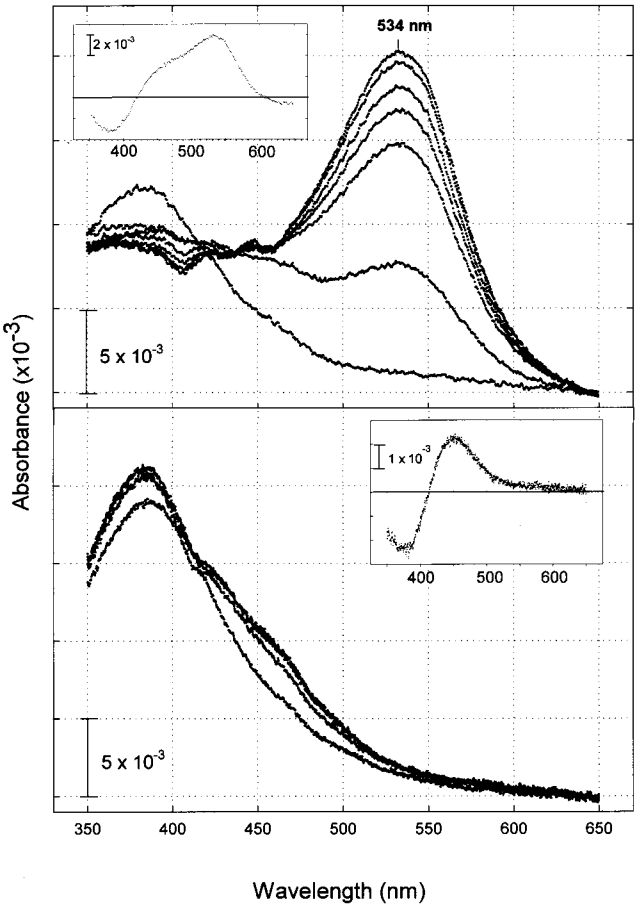

FIGURE 4: Absorption spectra of retinal-reconstituted NOP-1 in *P. pastoris* membranes compared to control membranes. *All-trans* retinal was added to a 2 mL membrane preparation of the *nop-1*-transformed strain L4 and the V1 strain transformed with the vector only. (Top panel) Spectra for the reconstitution of NOP-1 membranes showing from bottom to top at 534 nm selected time points: 0, 10, 40, 55, 70, 90, and 105 min. 0 min designates immediately after retinal addition. (Inset) Absorption difference spectrum of 10 min minus 0 min. (Bottom panel) Spectra for the reconstitution of V1 membranes at selected time points from bottom to top at 450 nm: 0, 10, 60, and 90 min. (Inset) Absorption difference spectrum of 10 min minus 0 min.

Coomassie staining of electrophoretically separated protein from a whole cell lysate of a *P. pastoris* transformant containing the *nop-1* gene revealed a protein at 30 kDa not

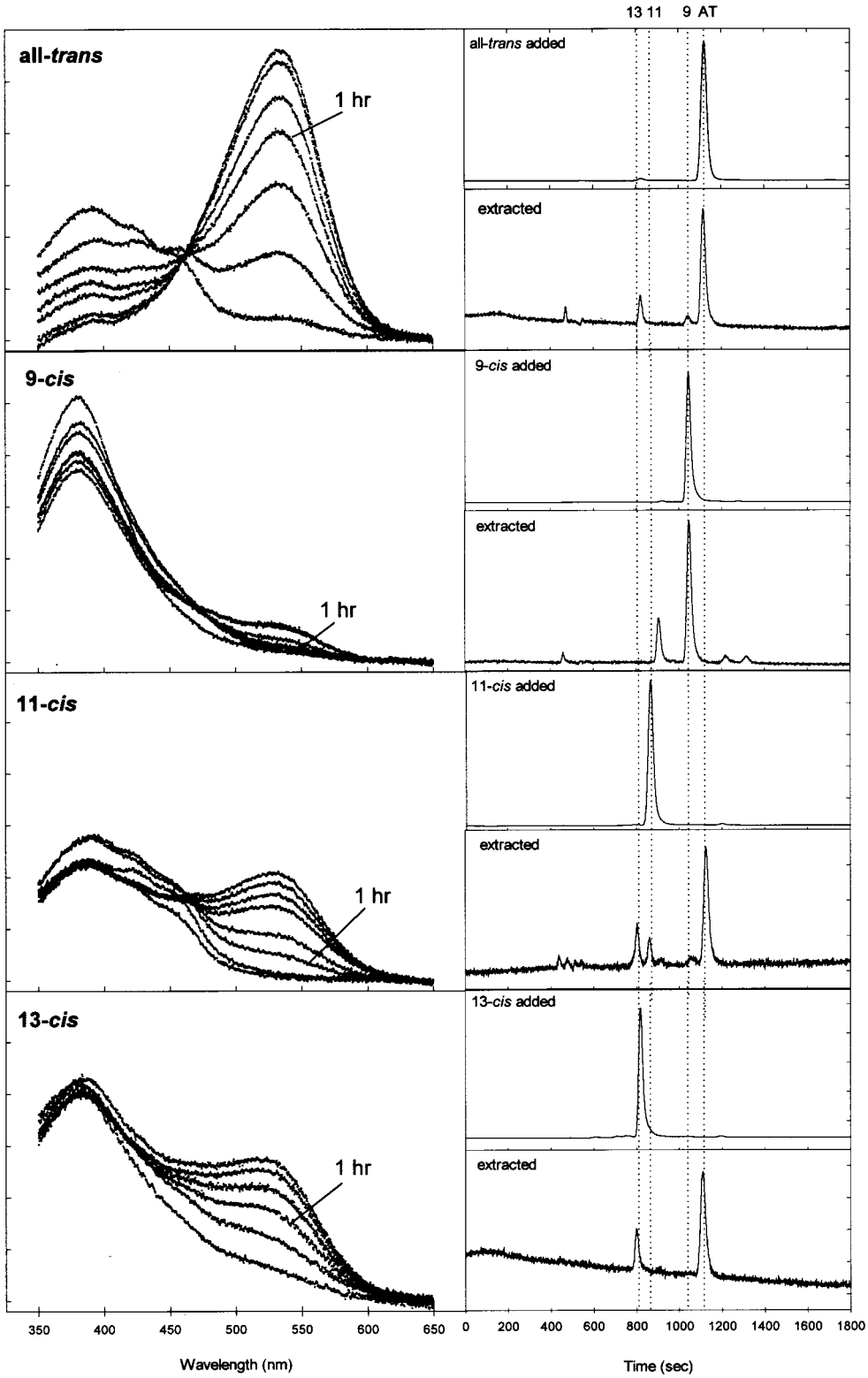

FIGURE 5: Reconstitution of NOP-1 in *P. pastoris* membranes with retinal isomers and subsequent retinal extraction. *All-trans*, 9-*cis*, 11-*cis*, and 13-*cis* retinals were added to 2 mL membrane suspensions and incubated in the dark at room temperature for 4 h. Membranes were immediately extracted and analyzed by HPLC to determine isomer content. The left column shows the absorption spectra monitoring reconstitution by each isomer. The distance between tick marks on the absorbance scale for each graph is 0.005. The absorption spectra shown from bottom to top at 530 nm are as follows: (*all-trans*) 0, 10, 30, 60, 90, 150, 180 min; (9-*cis*) 0, 10, 30, 60, 90, 150 min; (11-*cis*) 0, 10, 60, 90,150, 180, 210, 240 min; (13-*cis*) 0, 10, 30, 60, 120, 180 min. The right column shows HPLC chromatograms for the purified isomer stock solutions and the membrane isomer content after extraction at 4 h (see Materials and Methods). Chromatograms for the extracted samples were aligned on the basis of their injection peaks. The ordinate tick intervals for the purified isomers are $(0.5-1) \times 10^5$ mV and for the extracted samples are $(0.4-1) \times 10^3$ mV.

evident in a control strain transformed with vector lacking *nop-1* (Figure 2B). Furthermore, this band is highly enriched and is the most abundant protein present in membranes from the *nop-1* transformant L4, whereas no species migrating at this position is observed in the control strain (V1) membranes. Immunoblot analysis of the same samples (Figure

2B) using anti-his-tag antibody confirmed that the 30 kDa protein corresponds to the *nop-1* gene product, which was engineered to contain a C-terminal his-tag epitope.

To quantitate the concentration of NOP-1 in the *P. pastoris* membranes, we established a calibration curve of Coomassie density (Figure 3) using purified sensory rhodopsin I (*26*), a protein expected to exhibit similar affinity for Coomassie dye. On the basis of three determinations of NOP-1 amount using various dilutions of strain L4 membrane preparations, we obtained the average value of 0.17 mg of NOP-1 protein/mL of membrane preparation. This value corresponds to 2.2 mg of NOP-1 protein/L of yeast culture, which corresponds to 5−6% of the total membrane protein produced by yeast (*27*) and is over 8-fold higher yield than obtained for bovine opsin using a similar procedure (*21*).

NOP-1 Binds Retinal To Generate a Green-Absorbing Pigment. *All-trans* retinal was added to membrane preparations, and the absorption spectrum in the visible range was monitored. Within 10 min of addition, the free retinal peak at 370 nm was depleted with generation of absorption at longer wavelengths (Figure 4). In the 10 min spectrum a broad absorption increase is evident, with peak absorbance at 534 nm accompanied by a shoulder near 450 nm. With further incubation the 534 nm band increased and the shoulder disappeared. A peak near 450 nm similar to the shoulder is also observed when retinal is added to membranes not containing the NOP-1 protein. Therefore, this peak is not due to retinal complexation with NOP-1 but rather with endogenous lipids and proteins in *Pichia* membranes. The pigment absorbing at 534 nm is generated only in the membranes containing NOP-1 and is referred to below as NR_{534}. The lack of the green-absorbing peak in the control membranes verifies that no endogenous unreconstituted opsin was present in *P. pastoris* and that spectral changes are not due to retinal perturbation of existing pigments in the membrane. The ~100 nm half-bandwidth of NR_{534} is typical of retinylidene protein absorption spectra, and the red-shifted λ_{max} indicates a protonated Schiff base linkage of the retinal.

Assuming an extinction coefficient of 50 000 M^{-1} cm^{-1} for the 534 nm pigment, the absorption generated at 534 nm in a membrane preparation at 4.7 mg of protein/mL, which produced 3.5×10^{-2} absorbance units in 2 h, corresponded to pigment formation by 25% of the NOP-1 protein present in the membranes. This value is greater than that achieved for retinal reconstitution of bovine opsin expressed in this system (4−15% for different preparations; *21*).

Reconstitution with Retinal Isomers. Retinal in the *all-trans*, 9-*cis*, 11-*cis*, or 13-*cis* isomeric configurations was added to membranes containing NOP-1, and the absorption generated was monitored. *All-trans* retinal reconstituted the green-absorbing pigment most rapidly (Figure 5). 11-*cis* and 13-*cis* retinal isomers formed pigments indistinguishable from that produced by *all-trans*, but at severalfold slower rates. The 9-*cis* isomer formed negligible amounts of the pigment even after 4 h incubation. Extraction of the retinal from the *Pichia* membranes 4 h after addition of each purified isomer showed that the 11-*cis* and 13-*cis* isomers were converted primarily to the *all-trans* configuration during the reconstitution process (Figure 6). The 9-*cis* isomer, the only one that failed to generate substantial amounts of the green-absorbing pigment, is not converted to the *all-trans* configuration during the incubation period.

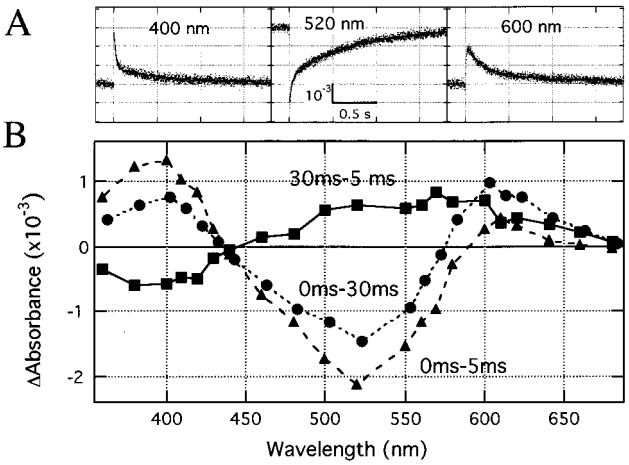

FIGURE 6: (A) Laser flash-induced absorption transients of NOP-1 in *P. pastoris* membranes. Membrane pellets at 23 °C were subjected to a 532 nm laser flash at time 0 and absorption changes were monitored at 1.0 ms per point at the indicated wavelengths. Two-exponential decay fits are drawn through the points. Rate constants: at 400 nm, 2.7 and 53 s^{-1}; at 520 nm, 1.5 and 38 s^{-1}; at 600 nm, 173 s^{-1} rise (line not drawn) and 4.1 s^{-1} decay. (B) Flash-induced absorption difference spectra of NOP-1. Laser flash-induced absorption transients of membrane pellets containing NOP-1 were collected as in (A) at various monitoring wavelengths. Symbols: triangles, absorption change amplitudes at 5 ms; circles, absorption change amplitudes at 30 ms; squares, difference spectrum of 30 ms minus 5 ms amplitude spectra.

The addition of retinal isomers to control membranes lacking NOP-1 showed that 11-*cis* and 13-*cis* isomers exhibit significant thermal isomerization to the *all-trans* configuration in the *Pichia* membrane, whereas 9-*cis* does not. Membrane-catalyzed thermal isomerization of 11-*cis* and 13-*cis*-retinal has been reported previously (*28*). Therefore, the formation of the 534 nm pigment after addition of 11-*cis* and 13-*cis* retinal may result from binding of *all-trans* retinal formed outside of the retinal binding pocket of NOP-1. Both the reconstitution rates and the extraction data strongly support that the isomeric configuration of the chromophore in the pigment generated by NOP-1 complexation with retinal is *all-trans*.

Retinal-Reconstituted NOP-1 Exhibits a Photochemical Reaction Cycle. Pellets of membranes containing the 534 nm *N. crassa* rhodopsin generated by *all-trans* retinal were subjected to a 532 nm laser flash and analyzed in the millisecond to second time window for photochemical reactivity. Transient flash-induced absorption depletion was observed near the absorption maximum of the pigment (520 nm trace, Figure 6), indicating a cyclic photochemical reaction sequence (photocycle). Absorption increases were detected at 400 and 600 nm, indicating photointermediate species with lifetimes in the seconds. Absorption difference spectra show that at 5 ms an intermediate with an absorption maximum near 400 nm is produced (Figure 6), typical of an unprotonated Schiff base form (M intermediate) of retinylidene pigments. The 30 ms minus 5 ms difference spectrum indicates that subsequently an intermediate species red-shifted from the unphotolyzed 534 nm state occurs in the photocycle (O intermediate).

The fast component at each of the three wavelengths of maximal change (400, 520, and 600 nm) fits a photocycle in which the 534 nm unphotolyzed state (NR_{534}) is converted

to M within the 0.8 ms resolution of the data acquisition system, followed by M → O in ~10 ms (responsible for the increase at 520 and 600 nm) and O → NR_{534} in 250−500 ms. O formation coincides with the fast M decay, but the slow M is not correlated with appearance of O. This could be explained by the presence of parallel pathways in which the fast M decays to O and the slow M decays to the 534 nm pigment without measurable accumulation of O, probably because the O decay is faster than that of slow M. Very similar behavior has been reported for transducer-free SRII in *Halobacterium salinarum* membranes at alkaline pH (*29*). An alternative explanation is that thermal back-reactions establishing equilibria between M, a subsequent intermediate N with an absorption spectrum similar to that of NR_{534}, and O (as described for bacteriorhodopsin; *30*) account for the mismatch between M decay and O rise. Although the kinetics are complex, the data indicate that, as in bacteriorhodopsin and sensory rhodopsins I and II, light induces transient deprotonation of the Schiff base.

CONCLUSION

Our results demonstrate that the *N. crassa* gene *nop-1* encodes a membrane protein that forms with *all-trans*-retinal a green light-absorbing pigment (λ_{max} 534 nm) with a spectral shape and bandwidth typical of archaeal rhodopsins. Laser flash kinetic spectroscopy demonstrates that the retinal-reconstituted pigment undergoes a photochemical reaction cycle with a near-UV-absorbing intermediate that is similar to the M intermediates produced by transient Schiff base deprotonation of the chromophore in the photocycles of bacteriorhodopsin and sensory rhodopsins I and II. The presence of both M-like and O-like species in a seconds-long photocycle is most closely similar to the photocycle of the phototaxis receptor sensory rhodopsin II (*29*).

The halobacterial rhodopsins fall into two distinct groups on the basis of their function: light-driven electrogenic ion transporters and light sensors for phototaxis (*31*). The former function independently of other proteins (*2*−*4*), while the latter function by protein−protein interaction with other membrane proteins (*32*), namely, the bound transducer proteins HtrI and HtrII (*33*, *34*). Primary sequence homology places the transport and sensory rhodopsins in two distinct phylogenetic subgroups (*35*). Phylogenetic analysis places NOP-1 as equally distant from each subgroup (*17*), and therefore we cannot assign the function of NOP-1 on the basis of its primary sequence. The flash photolysis results, however, do provide a clue. The transport rhodopsins are characterized by photocycles of ~10 ms, whereas sensory rhodopsins are slow-cycling pigments with lifetimes in the 100 ms to seconds range (*5*). This kinetic difference is functionally important since for a transporter a rapid photocycling rate is advantageous for efficient pumping, whereas a slower cycle provides more efficient light detection to a sensor since signaling states persist for longer times (*36*). The long lifetime of the M intermediate in the photocycle of NOP-1 therefore argues for a sensory function. One caveat is that the NOP-1 photocycle kinetics may be altered by heterologous expression in the non-native membrane environment. However, time-resolved absorption changes of bacteriorhodopsin in isolated plasma membrane from *Schizosaccharomyces pombe* showed rise and decay kinetics of the M intermediate during the photocycle similar to those observed in the homologous system (*37*).

Since the discovery of the light-driven proton pump bacteriorhodopsin nearly 30 years ago (*38*), ~30 homologous proteins have been described, all in archaeal halophilic prokaryotes (*35*). The presence of a photoactive member of this family in a eukaryote opens the possibility for a much broader distribution than previously realized.

ACKNOWLEDGMENT

We thank Kevin Ridge for his advice on the *P. pastoris* expression system.

REFERENCES

1. Baldwin, J. M., Schertler, G. F. X., and Unger, V. M. (1997) *J. Mol. Biol. 272*, 144−164.
2. Grigorieff, N., Ceska, T. A., Downing, K. H., Baldwin, J. M., and Henderson, R. (1996) *J. Mol. Biol. 259*, 393−421.
3. Lanyi, J. K. (1998) *J. Struct. Biol. 124*, 164−178.
4. Oesterhelt, D. (1998) *Curr. Opin. Struct. Biol. 8*, 489−500.
5. Hoff, W. D., Jung, K.-H., and Spudich, J. L. (1997) *Annu. Rev. Biophys. Biomol. Struct. 26*, 223−258.
6. Spudich, J. L., and Zacks, D. N. (1996) *Biomembranes 2A*, 199−226.
7. Lipson, E. D., and Horwitz, B. A. (1991) *Mod. Cell Biol. 10*, 1−64.
8. Hellingwerf, K. J., Hoff, W. D., and Crielaard, W. (1996) *Mol. Microbiol. 21*, 683−693.
9. Roenneberg, T., and Foster, R. G. (1997) *Photochem. Photobiol. 66*, 549−561.
10. Dunlap, J. C. (1999) *Cell 96*, 271−290.
11. Foster, K. W., Saranak, J., Patel, N., Zarilli, G., Okabe, M., Kline, T., and Nakanishi, K. (1984) *Nature 311*, 756−759.
12. Saranak, J., and Foster, K. W. (1997) *Nature 387*, 465−466.
13. Hegemann, P., Gartner, W., and Uhl, R. (1991) *Biophys. J. 60*, 1477.
14. Lawson, M. A., Zacks, D. N., Derguini, F., Nakanishi, K., and Spudich, J. L. (1991) *Biophys. J. 60*, 1490−1498.
15. Sakamoto, M., Wada, A., Akai, A., Ito, M., Goshima, T., and Takahashi, T. (1998) *FEBS Lett. 434*, 335−338.
16. Deininger, W., Kroger, P., Hegemann, U., Lottspeich, F., and Hegemann, P. (1995) *EMBO J. 14*, 5849−5858.
17. Bieszke, J. A., Braun, E. L., Bean, L. E., Kang, S., Natvig, D. O., and Borkovich, K. A. (1999) *Proc. Natl. Acad. Sci. U.S.A. 96*, 8034−8039.
18. Macino, G., Arpaia, G., Linden, H., and Bellario, P. (1998) in *Microbial Responses to Light and Time* (Caddick, M. X., et al., Eds.) pp 213−224, Cambridge University Press, Cambridge, U.K.
19. Carattoli, A., Kato, E., Rodriguez-Franco, M., Stuart, W. D., and Macino, G. (1995) *Proc. Natl. Acad. Sci. U.S.A. 92*, 6612−6616.
20. Lawson, M. A., Zacks, D. N., Derguini, F., Nakanishi, K., and Spudich, J. L. (1991) *Biophys. J. 60*, 1490−1498.
21. Abdulaev, N. G., Popp, M. P., Smith, W. C., and Ridge, K. (1997) *Protein Expression Purif. 10*, 61−69.
22. Borkovich, K. A., Farrelly, F. W., Finkelstein, D. B., Taulien, J., and Lindquist, S. (1989) *Mol. Cell. Biol. 9*, 3919−3930.
23. Spudich, E. N., Zhang, W., Alam, M., and Spudich, J. L. (1997) *Proc. Natl. Acad. Sci. U.S.A. 94*, 4960−4965.
24. Scherrer, P., Mathew, M. K., Sperling, W., and Stoeckenius, W. (1989) *Biochemistry 28*, 829−834.
25. Laroche, Y., Storme, V., De Meutter, J., Messens, J., and Lauwereys, M. (1994) *Biotechnology 12*, 1119−1124.
26. Krebs, M. P., Spudich, E. N., and Spudich, J. L. (1995) *Protein Expression Purif. 6*, 780−788.

27. Sekler, I., Kopito, R., and Casey, J. R. (1995) *J. Biol. Chem. 270*, 21028−21034.
28. Groenendijk, G. W., Jacobs, C. W., Bonting, S. L., and Daemen, F. J. (1980) *Eur. J. Biochem. 106*, 119−128.
29. Sasaki, J., and Spudich, J. L. (1999) *Biophys. J.* (in press).
30. Balashov, S. P., Lu, M., Imasheva, E. S., Govindjee, R., Ebrey, T. G., Othersen, B., III, Chen, Y., Crouch, R. K., and Menick, D. R. (1999) *Biochemistry 38*, 2026−2039.
31. Spudich, J. L. (1998) *Mol. Microbiol. 28*, 1051−1059.
32. Zhang, X.-N., Zhu, J., and Spudich, J. L. (1999) *Proc. Natl. Acad. Sci. U.S.A. 273*, 19722−19728.
33. Yao, V. J., and Spudich, J. L. (1992) *Proc. Natl. Acad. Sci. U.S.A. 89*, 11915−11919.
34. Zhang, W., Brooun, A., Mueller, M. M., and Alam, M. (1996) *Proc. Natl. Acad. Sci. U.S.A. 93*, 8230−8235.
35. Ihara, K., Umemura, T., Katagiri, I., Kitajima-Ihara, T., Sugiyama, Y., Kimura, Y., and Mukohata, Y. (1999) *J. Mol. Biol. 285*, 163−174.
36. Yan, B., Takahashi, T., and Spudich, J. L. (1991) *Biochemistry 30*, 10686−10692.
37. Hildebrandt, V., Ramezani-Rad, M., Swida, U., Wrede, P., Grzesiek, S., Primke, M., and Büldt, G. (1989) *FEBS Lett. 243*, 137−140.
38. Oesterhelt, D., and Stoeckenius, W. (1971) *Nat. New Biol. 233*, 149−152.

BI9916170